The compact Hα emitting regions of the Herbig Ae/Be stars HD 179218 and HD 141569 from CHARA spectro-interferometry

I. Mendigutía,[1][⋆] R. D. Oudmaijer,[1] D. Mourard[2] and J. Muzerolle[3]

[1]*School of Physics and Astronomy, University of Leeds, Woodhouse Lane, Leeds LS2 9JT, UK*
[2]*Université Côte d'Azur, OCA, CNRS, Lagrange, Parc Valrose, Bât. H. FIZEAU, F-06108 Nice cedex 02, France*
[3]*Space Telescope Science Institute, 3700 San Martin Dr., Baltimore, MD 21218, USA*

ABSTRACT

This work presents CHARA/VEGA Hα spectro-interferometry ($R \sim 6000$, and $\lambda/2B \sim 1$ mas) of HD 179218 and HD 141569, doubling the sample of Herbig Ae/Be (HAeBe) stars for which this type of observations is available so far. The observed Hα emission is spatially unresolved, indicating that the size of the Hα emitting region is smaller than $\sim$0.21 and 0.12 au for HD 179218 and HD 141529 ($\sim$15 and 16 R_*, respectively). This is smaller than for the two other HAeBes previously observed with the same instrumentation. Two different scenarios have been explored in order to explain the compact line emitting regions. A hot, several thousand K, blackbody disc is consistent with the observations of HD 179218 and HD 141569. Magnetospheric accretion (MA) is able to reproduce the bulk of the Hα emission shown by HD 179218, confirming previous estimates from MA shock modelling with a mass accretion rate of 10^{-8} $M_\odot$ yr^{-1}, and an inclination to the line of sight between 30° and 50°. The Hα profile of HD 141569 cannot be fitted from MA due to the high rotational velocity of this object. Putting the CHARA sample together, a variety of scenarios is required to explain the Hα emission in HAeBe stars – compact or extended, discs, accretion, and winds – in agreement with previous Brγ spectro-interferometric observations.

Key words: accretion, accretion discs – line: formation – techniques: interferometric – protoplanetary discs – stars: pre-main-sequence.

1 INTRODUCTION

Pre-main sequence (PMS) objects are optically visible young stars mostly surrounded by proto-planetary discs. Low- and intermediate-mass PMS stars (Classical T Tauri: CTT and Herbig Ae/Be stars: HAeBe, respectively) show IR excess from circumstellar discs and were primarily defined from the presence of the Hα line in emission, which is mainly associated with accretion and winds (Muzerolle, Hartmann & Calvet 1998; Kurosawa, Harries & Symington 2006; Lima et al. 2010; Tambovtseva, Grinin & Weigelt 2014).

Despite the presence of the Hα emission line is a defining characteristic of PMS stars, spatially resolved observations of this feature are very scarce. The bulk of the hydrogen recombination line is supposed to come from the inner parts of the disc at a few stellar radii from the central star, for which spectro-interferometric observations become crucial to investigate this. However, most of such studies have focused on the near-IR Brγ transition, mainly due to the wider access to near-IR interferometers. Brγ spectro-interferometry of an increasing number of PMS stars (around 20 bright and close HAeBes up to date, see e.g. Kraus 2015) reveals that the emission comes from a few stellar radii, generally tracing magnetospherically driven accretion, outflows and/or Keplerian discs (see e.g. Kraus et al. 2008; Eisner et al. 2010; Mendigutía et al. 2015; Kurosawa et al. 2016). Concerning Hα, the only spectro-interferometric observations in PMS stars were those obtained with the CHARA/VEGA interferometer (Mourard et al. 2009) for AB Aur (Rousselet-Perraut et al. 2010) and MWC 361 (Benisty et al. 2013). The results found for both HAeBe stars are consistent with a spatially resolved non-spherical wind. In a recently accepted paper, Perraut et al. (2016) revisit the problem on the Hα emission in AB Aur from CHARA data with improved sensitivity and spatial resolution. The new results confirm the disc-wind origin, although concluding that a magnetospheric accretion (MA) component cannot be completely neglected.

In this work, we present CHARA/VEGA spectro-interferometric observations in Hα for two additional HAeBes, HD 179218 and HD 141569, doubling the sample so far available with this type of observations. Since we find that the Hα emission is unresolved in these objects, physical scenarios other than extended winds are tested. Section 2 includes some properties of the target stars, Section 3 describes the observations and data reduction, Section 4 presents

⋆ E-mail: I.Mendigutia@leeds.ac.uk

Table 1. Properties of the stars.

Star	d	T_*	M_*	R_*	$v \sin i$	i
–	(pc)	(K)	(M$_\odot$)	(R$_\odot$)	(km s^{-1})	(°)
HD 179218	201 ± 24	9500 ± 500	2.6 ± 0.2	2.9 ± 0.9	72 ± 3	40 ± 10
HD 141569	112 ± 34	9750 ± 250	1.9 ± 0.4	1.5 ± 0.5	258 ± 17	56 ± 1

Notes. The distance, effective temperature, mass, and radius for HD 179218 and HD 141569 are from Montesinos et al. (2009) and Fairlamb et al. (2015), respectively; the projected rotational velocity from Guimarães et al. (2006) and Mora et al. (2001), and the inclination to the line of sight from Dent, Greaves & Coulson (2005) and Mayozer et al. (2016).

an analysis in terms of upper limits for the size of the line emitting regions, blackbody discs, and MA, and Section 5 summarizes the main conclusions.

2 TARGET STARS

Table 1 shows the distance, stellar temperature, mass, radius, projected rotational velocity, and inclination to the line of sight (90° for an edge-on and 0° for a pole-on disc) of HD 179218 and HD 141569. Both objects are young, bright (<10 Myr and R-magnitudes of 7.00 and 7.25, respectively; see Mendigutía et al. 2011b, and references therein), and they are relatively close by HAe (A0) stars with similar stellar properties, although HD 141569 is a fast rotator. Whereas the disc inclination for HD 141569 was inferred from spatially resolved observations, the one for HD 179218 has a larger degree of uncertainty, which could range from 0° to 45° (Liu et al. 2007; van der Plas et al. 2008). The corresponding value indicated in Table 1 comes from a simple model fit to the CO (J = 3–2) line profile.

HD 179218 is a group I object according to the Meeus et al. (2001) classification, with the near-IR (K band) already in excess and a stable, single-peaked Hα profile (Mendigutía et al. 2011a, 2012). The mass accretion rate is $<5 \times 10^{-8}$ M$_\odot$ yr^{-1} (Mendigutía et al. 2011b). A possible companion is located at $\sim$2.5 arcsec (Thomas et al. 2007; Wheelwright, Oudmaijer & Goodwin 2010, i.e. larger than the field of view covered from the interferometric observations). Fedele et al. (2008) showed that HD 179218 has two rings of dust at 1 and 20 au, and a compact gas emitting region between 1 and 6 au. A longitudinal magnetic field of 51 ± 30 G was measured by Hubrig et al. (2009).

HD 141569 is a Meeus group II star with an IR excess starting at wavelengths close to 10 μm and a stable, double-peaked Hα emission line with the red peak slightly less intense than the blue (Mendigutía et al. 2011a, 2012). The accretion rate is between $\sim$10^{-7} and 10^{-8} M$_\odot$ yr^{-1} (Mendigutía et al. 2011b; Fairlamb et al. 2015). The object has two low-mass stellar companions at wide distances (Weinberger et al. 1999, angular separations of 7.6 and 9 arcsec). The transitional nature of HD 141569 has been verified from direct imaging, showing a huge hole depleted of dust extending up to $\sim$100 au (Weinberger et al. 1999). The external disc shows two ring-like belts at $\sim$210 and 380 au and other structures (see Mayozer et al. 2016, and references therein) that could be indicative of the presence of giant planets (Wyatt 2005; Reche, Beust & Augereau 2009). An additional inner ring ($<$100 au), spatially coincident with warm gas, was recently reported by Konishi et al. (2016). A very weak or non-existent longitudinal magnetic field was reported by Wade et al. (2007) from several metallic lines.

3 OBSERVATIONS AND DATA REDUCTION

Observations of HD 179218 and HD 141569 were taken at the CHARA array with the VEGA spectrometer on 2015 July. The
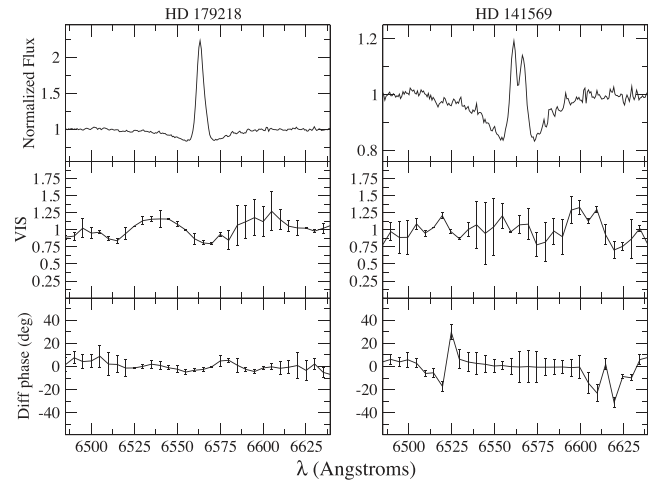
Figure 1. CHARA normalized Hα fluxes (note the different scales), visibilities, and differential phases for HD 179218 and HD 141569 taken with the 66 m E1E2 baseline.

wavelength range covered was 6300–6700 Å, at a spectral resolution $\sim$6000. The configurations used were S1S2, E1E2, and S2W2, with corresponding baselines of 34, 66, and 178 m. Calibration stars of similar spectral types and brightness (HD 181383 and HD 140075) were observed with the same observing configuration, using a CAL-SCI-CAL-SCI sequence with SCI exposure times of $\sim$25 min. Data reduction was carried out using the standard VEGA procedure (Mourard et al. 2009). The first processing is done using a large spectral band of 30 nm on which the spectral density of the short exposures are summed and the raw squared visibility is extracted. In all cases, we found that the target is unresolved in this large spectral band. The second processing concerns the computation of the differential visibility by computing the cross-spectrum between the same large band and a narrow band of 2 nm (equivalent spectral resolution of 320) moving across the large band. The differential visibility and differential phase are thus extracted and they help in putting constraints on the size and astrometric position of each small spectral band with respect to the large band. Instrumental artefacts were corrected for by dividing the observables of the target stars by those from the calibrators.

Data taken with the S1S2 and S2W2 baselines were finally rejected because of the low signal-to-noise ratio resulting from poor observing conditions on 2015 July 06 and 2015 July 12. The E1E2 observations were taken on 2015 July 07 and are of good quality. Fig. 1 shows the averaged results for the E1E2 baseline in terms of normalized Hα line fluxes, visibilities, and differential phases. Error bars for the visibilities and differential phases come from the standard deviation of the SCI frames. The on-sky position angles (from north to east) are 297°–305° and 300°–320° for HD 179218 and

HD 141569, respectively, the ranges coming from the spread in the *uv* coverage. The Hα profiles shown by HD 179218 and HD 141569 are single and double-peaked, respectively, the observed emission with an equivalent width (EW) of -8.47 ± 0.05 and -3.2 ± 0.2 Å. The Hα line remains practically unaltered from previous observations (e.g. Mendigutía et al. 2011a). The visibilities randomly oscillate around 1 ($\pm \sim 0.25$), without showing any significant difference between the continuum and the Hα line. This indicates that both the central stars and the line emitting regions are spatially unresolved. Similarly, the differential phases are randomly distributed around 0° (with errors up to $\sim \pm 20°$), showing no signs of asymmetries in the plane of the sky.

4 ANALYSIS

The fact that the Hα line is unresolved sets an initial constraint on the size of the emitting region. The smallest angular distance that can be resolved from our observations is given by $\lambda/2B \sim 1$ mas, with $\lambda = 6562.8$ Å, and B = 66 m (baseline E1E2). At the distance of the target stars, this angular resolution indicates that the extent of the Hα emitting region should be smaller than 0.21 au (15 R_*) for HD 179218, and ~ 0.12 au (16 R_*) for HD 141569. That extent would reduce to only $\sim 6 R_*$ for both stars if the visibilities obtained with the S2W2 baseline are considered, although this value should be taken with caution given the poor quality of the S2W2 data. These results contrast with the two HAeBes that have been previously resolved with CHARA. The Hα line of AB Aur was resolved even with a smaller baseline (34 m), indicating an extent of the line emitting region of at least ~ 2 mas, or ~ 0.3 au at 144 pc (Rousselet-Perraut et al. 2010). Regarding the binary MWC 361, Benisty et al. (2013) estimated that the size of the Hα emitting region is in between ~ 0.2 and ~ 0.6 au, depending on the position of the companion. Non-spherical or magnetically driven disc winds with a spatial extent larger than the disc truncation radius were invoked in those works to fit the observed properties of AB Aur and MWC 361. Two different physical scenarios that could explain the comparatively small Hα emitting regions of HD 179218 and HD 141569 are discussed in the following.

4.1 Blackbody disc

An additional constraint for the size of the Hα emitting region can be derived assuming that this is an optically thick line characterized by a single, blackbody temperature $T_{H\alpha}$. The line luminosity can then be estimated from the integration of Planck's law, and can be expressed as $L_{H\alpha} = \epsilon A_{H\alpha} \sigma T_{H\alpha}^4$, with $A_{H\alpha}$ the projected area of the line emitting region, σ the Stefan–Boltzmann constant, and $0 \leq \epsilon \leq 1$ a correction factor that takes into account that the integration is carried out across the full width of the line. The value for ϵ can be derived numerically since

$$\epsilon = \frac{15}{\pi^4} \int_{u_2}^{u_1} \frac{u^3 du}{e^u - 1}; u_i = \frac{hc}{\lambda_i k T_{H\alpha}}, \quad (1)$$

with λ_1 and λ_2 the shortest and longest wavelengths where the Hα emission extends, and h, c, and k Planck's constant, the speed of light, and Boltzmann's constant, respectively. Since the stellar luminosity is $L_* = A_* \sigma T_*^4$, we have that $L_{H\alpha}/L_* = \epsilon(A_{H\alpha}/A_*)(T_{H\alpha}/T_*)^4$. The line-to-stellar luminosity ratio can also be expressed as $L_{H\alpha}/L_* = (d/R_*)^2(F_0 EW/\sigma T_*^4)10^{-0.4m}$, with EW the line equivalent width, m the R-magnitude characterizing the continuum adjacent to the Hα line and F_0 the corresponding zero-magnitude flux (taken from Bessell 1979). From the two

previous expressions for $L_{H\alpha}/L_*$, the ratio between the area of the line emitting region and that of the star can be derived as $A_{H\alpha}/A_* = (F_0 EW10^{-0.4m}/\sigma\epsilon T_{H\alpha}^4)(d/R_*)^2$. Finally, the radial extent of the Hα emitting region depends on the geometry assumed. If Hα is emitted in an inclined disc extending from the stellar surface (assumed spherical) up to a stelleocentric radius $r_{H\alpha}$, then this is given by

$$r_{H\alpha} = R_* \sqrt{\sqrt{\frac{F_0 EW10^{-0.4m}}{\sigma\epsilon T_{H\alpha}^4 \cos i} \frac{d^2}{R_*^2}} + 1}. \quad (2)$$

Other possible geometries for the line emitting region – e.g. spherical – provide smaller values of $r_{H\alpha}$.

Despite the simplicity of the assumptions, equation (2) is similar to the radius of the inner gaseous discs that has been successfully used to explain the hydrogen emission of super giants, classical Be stars and, more recently, of early-type HAeBe stars (see e.g. Grundstrom & Gies 2006; de Wit et al. 2008; Patel, Sigut & Landstreet 2016, and references therein). A more realistic model would include a range of temperatures and optical depths, although the assumption of a single blackbody temperature should be enough to roughly describe an inner disc emitting an optically thick line such as Hα. Indeed, a dependence of the previous expression is the temperature characterizing the line emitting region, $T_{H\alpha}$. In principle, this is a free parameter that should lie within several thousand kelvin for hydrogen to be at least partially ionized. For $T_{H\alpha} = T_*$, the total projected lengths of the Hα emitting region ($\sim 2r_{H\alpha}$) should be $\sim 2.5 R_*$ for both stars. This is below the spatial resolution limit of the baselines considered in this work, and therefore consistent with our observations. Higher temperatures would decrease $r_{H\alpha}$, whereas only very low, unlikely $T_{H\alpha}$ temperatures (<4000 K) would allow us to spatially resolve the Hα line emitting region. As a consequence, we conclude that a compact gaseous disc emitting like a blackbody at a temperature of several thousand kelvin could in principle be responsible of the Hα emission for both HD 179218 and HD 141569. In addition, a double-peaked line profile like the one shown by HD 141569 is characteristic of Keplerian-rotating discs. The peak emissions are located at around ± 115 km s^{-1}. This velocity corresponds to a Keplerian distance as close as $\sim 5 R_*$, where uncertainties from the spectral resolution and the error bars for the stellar masses and radii in Table 1 have also been taken into account. A homogeneous disc would produce a double-peaked line profile with similar peak intensities, thus the fact that the red peak is less intense than the blue could in principle be explained from differences in density between both sides of the rotating disc. However, the Hα profile of HD 141569 is roughly stable on time-scales ranging from several days to almost two decades (see Mendigutía et al. 2011a), which challenges the Keplerian disc as the only explanation for the Hα emission. A relatively constant infall of material would cause a red-shifted absorption which could explain why the red peak is always less intense than the blue. The inverse P-Cygni feature superimposed on some of the double-peaked Hα profiles shown in Mendigutía et al. (2011a) (not apparent in our CHARA observations) is consistent with this explanation. Given that the inclination estimated for HD 179218 indicates that this system is closer to pole-on (Section 4.2), a possible Keplerian disc could not be reflected by a characteristic double-peaked emission as the one shown by HD 141 569, which is closer to edge-on.

The previous procedure was repeated for the two other HAeBes resolved by CHARA in order to test whether their Hα emission could also be consistent with the blackbody disc model. Equation (2) indicates that the corresponding projected size for AB Aur would be ~ 0.04 au (3.2 R_*), i.e. an order of magnitude smaller than

inferred from CHARA observations (Rousselet-Perraut et al. 2010). Apart from the distance and inclination indicated in this paper, we have assumed the stellar temperature ($=T_{\mathrm{H}\alpha}$) and radius in Donehew & Brittain (2011) and the Hα parameters in Costigan et al. (2014). Once again, only for unrealistically low $T_{\mathrm{H}\alpha}$ temperatures (<3000 K), the blackbody disc could have been spatially resolved. Regarding MWC 361, the corresponding projected disc size would be ∼0.08 au (2.4 R_*), which is also an order of magnitude smaller than obtained from CHARA (Benisty et al. 2013). The data necessary to apply equation (2) were taken from that paper and from Hernández et al. (2004). It is noted that in this case Hα temperatures up to 6000 *K* could make the blackbody disc large enough to be resolved. In conclusion, given the small emitting size compared to the one derived from CHARA, the blackbody disc hypothesis is not consistent with the observed properties of AB Aur, in contrast to our target stars. In the case of MWC 361, a 'cold' blackbody disc with a temperature up to ∼6000 K could also explain that Hα is spatially resolved in this object.

4.2 Magnetospheric accretion

A major constraint of the MA scenario is that the Hα emission line is generated in the magnetosphere, in magnetically driven flows at a radial distance not further than the co-rotation radius (Shu et al. 1994). For the stellar parameters, projected rotational velocities and inclinations assumed here (Section 2), the co-rotation radii are 2.39 R_* and 1.36 R_* for HD 179218 and HD 141569, well below the radial extent that can be resolved with CHARA. There are only two previous examples in the literature for which MA has been used to reproduce the Hα emission shown by HAeBes (UX Ori and BF Ori in Muzerolle et al. 2004; Mendigutía et al. 2011b, respectively). H I line profiles in the near-IR of the HAeBe stars VV Ser and HD 58647 were also successfully reproduced from combined MA-wind models by Garcia Lopez et al. (2015) and Kurosawa et al. (2016), respectively (see also Tambovtseva, Grinin & Weigelt 2014, 2016). The remaining lines of evidence supporting that MA could work at least for several HAeBes mainly come from MA shock modelling of the near-UV excess (Muzerolle et al. 2004; Mendigutía et al. 2011b; Fairlamb et al. 2015), spectro-polarimetry (Vink et al. 2002; Mottram et al. 2007), and statistical analysis of line profiles (Cauley & Johns-Krull 2014, 2015).

In order to establish whether MA is able to reproduce the Hα profiles of HD 179218 and HD 141569, we have applied the line modelling described in Muzerolle, Calvet & Hartmann (2001). Specific details can be consulted there (see also Muzerolle et al. 2004; Mendigutía et al. 2011b), but a general description is included in the following. The model calculates the atomic level populations of free-falling gas channelled along magnetic field lines in a dipolar, axisymmetric field emerging from the star. Input data are the stellar parameters (M_*, R_*, T_*), the mass accretion rate ($\dot{M}_{\mathrm{acc}}$), the maximum temperature of the gas ($T_{\mathrm{H}\alpha}^{\mathrm{max}}$), the inclination ($i$), and the size of the magnetosphere in terms of the minimum and maximum radial distances from which the gas is channelled (r_{mi} and r_{ma}; see fig. 1 in Muzerolle et al. 2001). The stellar parameters and inclinations used for the modelling are those in Table 1, the mass accretion rates were varied within the limits provided by Mendigutía et al. (2011b) and Fairlamb et al. (2015) from MA shock modelling (Section 2), r_{ma} was fixed to the co-rotation radius, and r_{mi} was varied as a free parameter. Regarding $T_{\mathrm{H}\alpha}^{\mathrm{max}}$, the actual physics involved in heating the gas is still not understood, so this remains the least well constrained of all the parameters. As a first-order approach, it has been assumed that $T_{\mathrm{H}\alpha}^{\mathrm{max}}$ is similar within a few hundred kelvin to
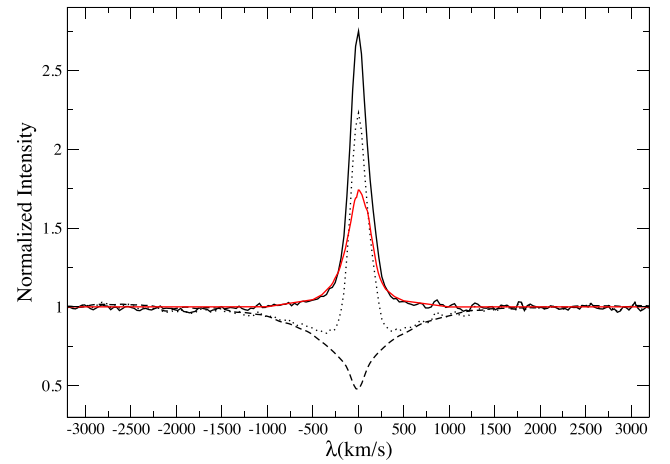

Figure 2. The observed Hα spectrum HD 179218 is indicated with the dotted line; the photospheric and the non-photospheric contributions with dashed and solid lines, respectively. The result from MA modelling is indicated with the red line (see text).

the MA shock temperatures provided in Mendigutía et al. (2011b) and Fairlamb et al. (2015) for HD 179218 and HD 141569, which is similar to the gas temperatures in the top of the range found for TTs (Muzerolle et al. 2001). We refer the reader to Muzerolle et al. (2001) and Muzerolle et al. (2004), where the influence of the different input parameters on the shape of the modelled line profiles were extensively discussed.

Fig. 2 shows the results of this modelling for HD 179218. The Hα profile observed with CHARA is plotted with a dotted line and includes the contribution of the photospheric absorption. This has been removed using a Kurucz synthetic profile corresponding to a star with the same effective temperature, surface gravity, and rotational velocity (dashed line). The resulting, non-photospheric Hα line is indicated with a black solid line. The best-fitted model is plotted with a red, solid line. The corresponding model parameters are the ones in Table 1, and $\dot{M}_{\mathrm{acc}} = 1.7 \times 10^{-8}$ M$_\odot$ yr^{-1}, $T_{\mathrm{H}\alpha}^{\mathrm{max}}$ = 13000 K, $r_{\mathrm{mi}} = 2.35\,R_*$, $r_{\mathrm{ma}} = 2.40\,R_*$. The modelled peak emission is smaller than observed (although larger fluxes result from inclinations smaller than 40°, see below). The radiative transfer methodology (using the Sobolev approximation) may break down in the densest, lowest velocity part of the flow, which may affect the poor fit near the line centre. However, MA modelling is not only able to reproduce at least ∼60 per cent of the non-photospheric Hα flux of HD 179218, but also fits the observed line wings. This indicates that MA is able to explain the bulk of the Hα emission in this object, and specially the high-velocity component. It is noted that the Hα broadening is strongly influenced by the Stark effect, for which models alternative to MA may also be able to reproduce the line wings as far as they include hot enough emitting regions. Remarkably enough, the current MA line modelling is consistent with the previous MA shock modelling of this star (Mendigutía et al. 2011b), both providing the same values for $\dot{M}_{\mathrm{acc}}$ and $T_{\mathrm{H}\alpha}^{\mathrm{max}}$. Moreover, MA line modelling confirms the inclination derived for this object by Dent et al. (2005). Fig. 3 shows that despite low inclinations ($i < 30°$) produce larger fluxes more similar than observed, the resulting peak emission is redshifted. On the other hand, Hα models with high inclinations (>50°) are blueshifted and do not fit the red wing of the line, even showing inverse P-Cygni profiles for edge-on configurations ($i > 70°$).

Regarding HD 141569, not only the corresponding range of input parameters mentioned above are unable to reproduce the observed
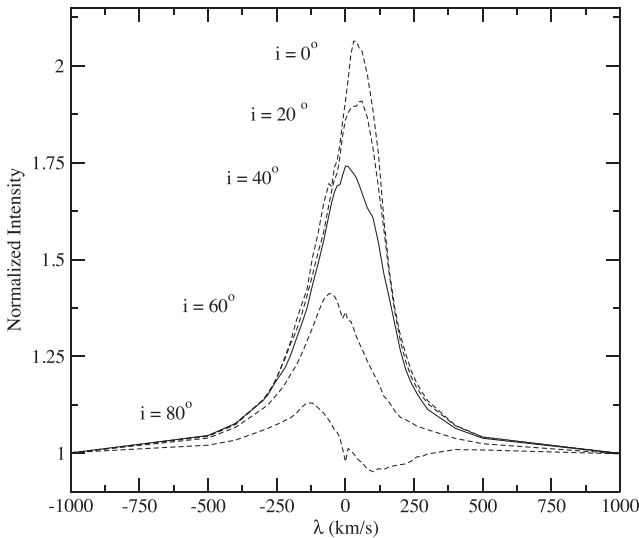
Figure 3. The previous modelled line profile for HD 179218 (solid line), considering additional inclinations to the line of sight (dashed lines), as indicated.

Hα profile, but apparently no set of input parameters can do it. Variations in the mass accretion rates of several orders of magnitude, changes in $T_{H\alpha}^{max}$ of several thousand kelvin, and a wide range of possible r_{mi} values have been attempted without success. As discussed in Muzerolle et al. (2004) (see also Mendigutía et al. 2011b), very high stellar rotation rates as the one shown by HD 141569 (Table 1) are problematic for the MA model used. Those rotational velocities result in very small co-rotation radii, for which the emission volume associated with such a small accretion flow is not enough to match the observed Hα emission regardless of any other combination of parameters. As argued by Muzerolle et al. (2004), geometries deviating from a standard dipole may reproduce the observations. Therefore, further theoretical development on how MA line modelling could deal with high rotational velocities (typically, $v \sin i > 150$ km s^{-1}) is necessary.

In spite of these results, we confirm that MA cannot be the primary origin of Hα emission in the two other HAeBes previously observed with CHARA. If the bulk of the line emission in AB Aur and MWC 361 were mainly generated in the magnetosphere, the line emitting region would even be smaller than in the previous, blackbody disc case, for which it would have been impossible to spatially resolve the line as it was done by Rousselet-Perraut et al. (2010) and Benisty et al. (2013). Moreover, a P-Cygni Hα profile such as the one shown by AB Aur is clearly inconsistent with accretion. As argued by Rousselet-Perraut et al. (2010), a full spherical wind providing matter along the line of sight would produce too much blueshifted absorption with respect to the observed P-Cygni feature, leaving the X-disc or disc-wind geometry as the best-suited scenario.

5 CONCLUSIONS

Our Hα interferometric observations of the HAeBe stars HD 179218 and HD 141569 add to the two previously reported (AB Aur and MWC 361), revealing that different phenomena could be originating the emission in this type of objects. The line can be emitted in a very compact region of a few stellar radii from hot blackbody discs (HD 179218 and HD 141569). The bulk of the Hα emission can be explained from MA in the case of HD 179218, but the current model cannot deal with high rotational velocities as the one shown

by HD 141569. A more extended emission can be explained from non-spherical winds (AB Aur and MWC 361), but a cold blackbody disc could also cause the Hα line of MWC 361. Despite the small sample of HAeBes that can be observed with current optical spectro-interferometric instrumentation, the variety reported matches with previous observations of the Brγ transition over a wider sample, where depending on the star the emission can also be compact, extended, associated with discs, accretion, or winds.

REFERENCES

Benisty M. et al., 2013, A&A, 555, A113
Bessell M. S., 1979, PASP, 91, 589
Cauley P. W., Johns-Krull C. M., 2014, ApJ, 797, 112
Cauley P. W., Johns-Krull C. M., 2015, ApJ, 810, 5
Costigan G., Vink J. S., Scholz A., Ray T., Testi L., 2014, MNRAS, 440, 3444
de Wit W. J., Oudmaijer R. D., Groenewegen M. A. T., Hoare M. G., Malbet F., 2008, A&A, 480, 149
Dent W. R. F., Greaves J. S., Coulson I. M., 2005, MNRAS, 359, 663
Donehew B., Brittain S., 2011, AJ, 141, 46
Eisner J. A. et al., 2010, ApJ, 718, 774
Fairlamb J. R., Oudmaijer R. D., Mendigutía I., Ilee J. D., van den Ancker M. E., 2015, MNRAS, 453, 976
Fedele D. et al., 2008, A&A, 491, 809
Garcia Lopez R., Kurosawa R., Caratti o Garatti A., Kreplin A., Weigelt G., Tambovtseva L. V., Grinin V. P., Ray T. P., 2016, MNRAS, 456, 156
Grundstrom E. D., Gies D. R., 2006, ApJ, 651, L53
Guimarães M. M., Alencar S. H. P., Corradi W. J. B., Vieira S. L. A., 2006, A&A, 457, 581
Hernández J., Calvet N., Briceño C., Hartmann L., Berlind P., 2004, AJ, 127, 1682
Hubrig S. et al., 2009, A&A, 502, 283
Konishi M. et al., 2016, ApJ, 818, L23
Kraus S., 2015, Ap&SS, 357, 97
Kraus S. et al., 2008, A&A, 489, 1157
Kurosawa R., Harries T. J., Symington N. H., 2006, MNRAS, 370, 580
Kurosawa R. et al., 2016, MNRAS, 457, 2236
Lima G. H. R. A., Alencar S. H. P., Calvet N., Hartmann L., Muzerolle J., 2010, A&A, 522, A104
Liu W. M., Hinz P. M., Meyer M. R., Mamajek E. E., Hoffmann W. F., Brusa G., Miller D., Kenworthy M. A., 2007, ApJ, 658, 1164
Mazoyer J. et al., 2016, ApJ, 818, 150
Meeus G., Waters L. B. F. M., Bouwman J., van den Ancker M. E., Waelkens C., Malfait K., 2001, A&A, 365, 476
Mendigutía I., Eiroa C., Montesinos B., Mora A., Oudmaijer R. D., Merín B., Meeus G., 2011a, A&A, 529, A34
Mendigutía I., Calvet N., Montesinos B., Mora A., Muzerolle J., Eiroa C., Oudmaijer R. D., Merín B., 2011b, A&A, 535, A99
Mendigutía I., Mora A., Montesinos B., Eiroa C., Meeus G., Merín B., Oudmaijer R. D., 2012, A&A, 543, A59
Mendigutía I., de Wit W. J., Oudmaijer R. D., Fairlamb J. R., Carciofi A. C., Ilee J. D., Vieira R. G., 2015, MNRAS, 453, 2126
Montesinos B., Eiroa C., Merín B., Mora A., 2009, A&A, 495, 901
Mora A. et al., 2001, A&A, 378, 116

Mottram J. C., Vink J. S., Oudmaijer R. D., Patel M., 2007, MNRAS, 377, 1363

Mourard D. et al., 2009, A&A, 508, 1073

Muzerolle J., Hartmann L., Calvet N., 1998, AJ, 116, 455

Muzerolle J., Calvet N., Hartmann L., 2001, ApJ, 550, 944

Muzerolle J., D'Alessio P., Calvet N., Hartmann L., 2004, ApJ, 617, 406

Patel P., Sigut T. A. A., Landstreet J. D., 2016, ApJ, 817, 29

Perraut K. et al., 2016, A&A, in press

Reche R., Beust H., Augereau J. C., 2009, A&A, 493, 661

Rousselet-Perraut K. et al., 2010, A&A, 516, L1

Shu F., Najita J., Ostriker E., Wilkin F., 1994, ApJ, 429, 781

Tambovtseva L. V., Grinin V. P., Weigelt G., 2014, A&A, 562, A104

Tambovtseva L. V., Grinin V. P., Weigelt G., 2016, A&A, 590, A97

Thomas S. J., van der Bliek N. S., Rodgers B., Doppmann G., Bouvier J., 2007, in Hartkopf W. I., Guinan E. F., Harmanec P., eds, Proc. IAU Symp., 240, Binary Stars as Critical Tools & Tests in Contemporary Astrophysics. Cambridge Univ. Press, Cambridge, p. 250

van der Plas G., van den Ancker M. E., Fedele D., Acke B., Dominik C., Waters L. B. F. M., Bouwman J., 2008, A&A, 485, 487

Vink J. S., Drew J. E., Harries T. J., Oudmaijer R. D., 2002, MNRAS, 337, 356

Wade G. A., Bagnulo S., Drouin D., Landstreet J. D., Monin D., 2007, MNRAS, 376, 1145

Weinberger A. J., Becklin E. E., Schneider G., Smith B. A., Lowrance P. J., Silverstone M. D., Zuckerman B., Terrile R. J., 1999, ApJ, 525, L53

Wheelwright H. E., Oudmaijer R. D., Goodwin S. P., 2010, MNRAS, 401, 1199

Wyatt M. C., 2005, A&A, 440, 937

This paper has been typeset from a TEX/LATEX file prepared by the author.